The interplay between photo-and radiation-induced darkening in ytterbium-doped fibres

Jean-Bernard Duchez, Franck Mady, Yasmine Mebrouk, Nadège Ollier, Mourad Benabdesselam

The interplay between photo- and radiation-induced darkening in ytterbium-doped fibres

Jean-Bernard DUCHEZ,[1,*] Franck MADY,[1] Yasmine MEBROUK,[1] Nadège OLLIER,[2] Mourad BENABDESSELAM[1]

[1] University of Nice Sophia Antipolis, Laboratoire de Physique de la Matière Condensée CNRS UMR 7336, Parc Valrose, 06108 NICE cedex 2, France
[2] Laboratoire des Solides Irradiés, UMR 7642, CEA-CNRS-Ecole Polytechnique, 91128 Palaiseau, France
**Corresponding author: jbduchez@unice.fr*

Received Month X, XXXX; revised Month X, XXXX; accepted Month X, XXXX; posted Month X, XXXX (Doc. ID XXXXX); published Month X, XXXX

This letter demonstrates a remarkable interplay between photo- and radiation-induced darkening of ytterbium-doped alumino-silica optical fibres operated in amplifying conditions and harsh environments (as e.g. in space-based applications). Influences of the pump power, ionizing dose and dose rate on this interaction are characterized. The pump is capable of accelerating or slowing-down the radiation-induced darkening build-up depending on the ionizing dose. The steady state photo-radio-darkening level is independent of the dose and at least equal to the equilibrium level of pure photo-darkening. This lower limit is notably reached at low dose rates, including those encountered in space. We therefore argue that photo-resistant ytterbium-doped fibres will resist against a space mission, whatever the dose.
OCIS Codes:140.3510, 140.3615, 160.2750, 160.5690, 160.6030, 260.5210, 350.5610.
http://dx.doi.org/10.1364/OL.99.099999

Ytterbium-doped silica optical fibres (YDF) serve to design efficient high output power laser sources used for cutting, welding, surgery, signal transmissions (free space optical links), or remote sensing (light detection and ranging: LIDAR). Due to their reduced weight, size and power consumption, YDF-based lasers offer a most appealing technology to implement, e.g., optical links and LIDAR in satellites or spacecrafts. Their development is however limited by the fact that YDF suffer from twofold degradation when operated in amplifying conditions and harsh radiative environments (as space). Excess optical losses can be induced by external ionizing radiations (radiation-induced darkening or RD), but also due to the pump (photo-darkening, PD). PD and RD have been examined separately so far, by distinct communities. PD has been well characterized [1-5] even if its origin and mechanism remain controversial [5]. RD has been rather poorly addressed in YDF [5,6] compared with erbium-doped fibres [7,8]. The possible interplay between PD and RD has not been clearly examined to date, though pump and ionizing radiations will act simultaneously in space operation conditions. This letter presents a detailed characterization of simultaneous photo-radiation-induced darkening (PRD) as a function of pump power, total ionizing dose and dose rate. Major constructive or destructive superimposition effects are demonstrated and discussed.

The measurement setup, based on a standard pump-probe scheme [2,9], is shown in Fig. 1. The fibre under test (FUT) is in-core pumped at 976 nm (input power ~250 mW) and a contra-propagative probe at 633 nm is used (a few mW). The bench allows in-line (under pumping) irradiations of the FUT by 45 kV x-rays from a copper-anode Inel XRG 3500 generator. FUTs consisted of ~2 cm long uncoated samples to ensure uniform inversion of Yb^{3+} ions (pump power is almost constant along the sample). Dose rates and doses given to the FUTs were monitored by an ionization chamber (PTW 23342 with electrometer UnidosE), placed right below the sample. In what follows we thus give actual values rather than targeted ones. Pump and probe beams are supplied by temperature and fibre-Bragg grating stabilized laser diodes (LD). Wavelength division multiplexers (WDM) are employed to couple pump and probe lights into the FUT. A set of 4 power-meters (PM) serve to estimate launched (PM 1 and 2) and transmitted (PM 3 and 4) powers at 976 and 633 nm respectively.

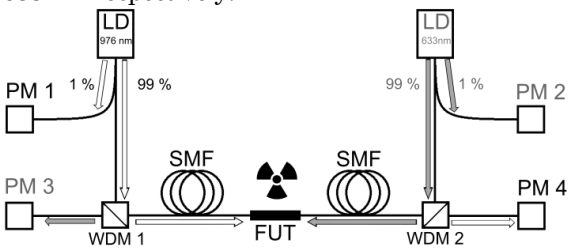

Fig. 1. Experimental setup for the characterization of PD, RD and simultaneous PRD.

Two aluminosilicate YDF have been compared. Their main characteristics are listed in Table 1. The K10 fibre was fabricated in our laboratory by modified chemical vapor deposition (MCVD) and solution doping. This 'classic' YDF is not optimized to resist against PD or RD. The Yb1200-4/125 fibre is a state-of-the-art commercial YDF manufactured by Liekki by the so-called direct nanoparticle deposition (DND) process. It offers low PD levels but probably contains additional co-dopants beyond aluminum.

Table 1. Characteristics of the investigated YDF.

YDF name	K10	Yb1200
Core/clad diameter (μm)	7.6/125	4/125 *
Numerical aperture	0.11	0.2 *
Absorption @976 nm (dB m-1)	575	1200 *
Yb conc. (cm^{-3}/at%)	4.5×10^{19}/0.13	9.4×10^{19}/u.v.
Al conc. (cm^{-3}/at%)	1.6×10^{20}/0.47	u.v.

*nominal values from manufacturer
u.v. = undisclosed values

The effect of the pump on fresh and photo-radio-darkened K10 samples is illustrated in Fig. 2 which displays the evolution of the pump output power normalized with respect to its initial value. Results are similar for the Yb1200 fibre. The upper curve corresponds to pure PD (pump input power P_{in} = 250 mW for >16 hours). The 976 nm FUT transmission decays due to PD and tends towards a PD equilibrium level (PDEL) around 0.82 (18% transmission loss). Such a PDEL has been evidenced already [2] and shown to increase with inversion of Yb^{3+} ions, so pump power [2]. The PD level stabilizes because the pump is responsible for PD, but also for a balancing photo-bleaching (PB) effect. The lower curve was recorded by submitting a fresh K10 sample to PRD (pumping and x-ray irradiation) for 900 s (340 krad) before leaving the FUT to the sole action of the pump for > 22 hours. Due to the high dose rate (22.7 krad min^{-1}) the FUT output power decays rapidly in the PRD stage. RD largely dominates the PRD kinetics. At the end of PRD, the pump bleaches the fibre: its transmission tends remarkably towards the PDEL. Therefore the pump is also capable of bleaching RD. This is readily understandable from [5] where we demonstrated that color centers responsible for PD and RD are the same.

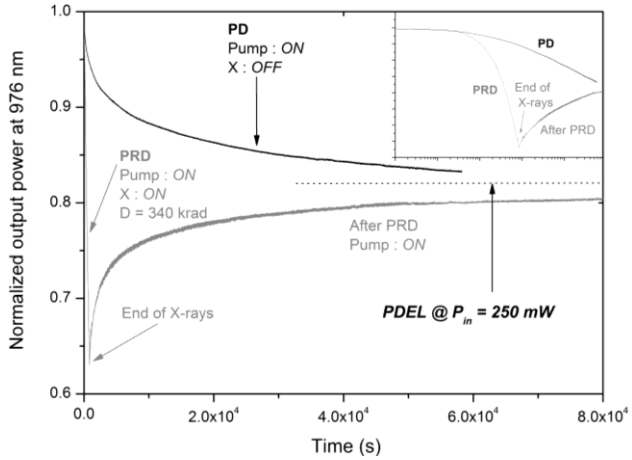

Fig. 2. Normalized output power at 976 nm for K10 samples for pure PD, and PRD followed by PB. Pump input power is P_{in} = 250 mW. Inset: same graphs in logarithmic scales to enlarge the PRD region.

Similar experiments were conducted at 2 additional doses (45, 150 krad) on fresh K10 samples. Fig. 3(a) and (b) display the normalized transmission at 976 and 633 nm respectively. PD plots are also shown. For the 2 higher doses, the result is the same as in Fig. 2, namely PRD followed by pump-induced PB. When x rays are stopped at 45 krad, the output power is still above the PDEL and the pump is responsible for further degradation, i.e. PD. All plots tend to the PDEL. The primary action of the pump (PD or PB) therefore depends on the ionizing dose! We always observed identical behaviors at pump and probe wavelengths, even if the degradation is – as usual – much higher in the visible range. To focus on the near-infra-red region, we hereafter report on losses induced at 976 nm only.

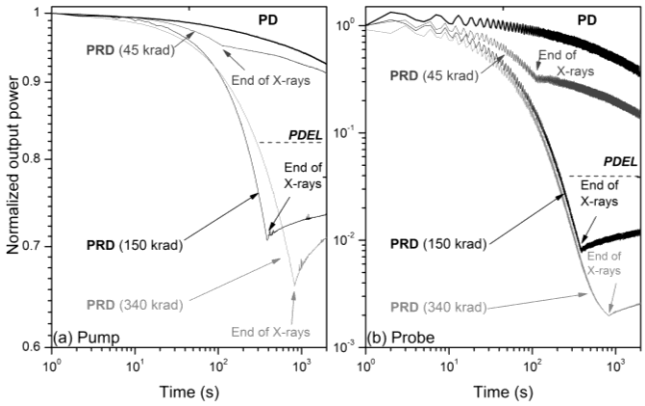

Fig. 3. Normalized output powers at 976 nm (a) and 633 nm (b) for pure PD and PRD at various doses (see plots) followed by PD or PB. Input pump power is P_{in} = 250 mW.

We now examine the role of the pump during x-ray irradiation. Doses of 30 krad and 450 krad were given to K10 and Yb1200 fibre samples. Each irradiation was repeated twice on fresh samples: one with the pump on (P_{in} = 250 mW), the other by keeping the pump off. Results are shown in Fig. 4. Data are plotted in terms of the excess absorption coefficient Δα(t) calculated according to equation (1) where L = 2 cm is the FUT length.

$$\Delta\alpha(t) = -\frac{1}{L}\times\ln\left(\frac{P_{out}(t)}{P_{in}(t)}\times\frac{P_{in}(0)}{P_{out}(0)}\right) \qquad (1)$$

$P_{in}(t)$ and $P_{out}(t)$ are input and output powers at 976 nm and time t. P_{in} is a priori constant, but small drifts might have to be corrected. Graphs are divided into 3 phases. In the early one, x rays are off and the pump is turned on for 10 s to measure its initial transmission level. In the second stage, x rays are turned on. The pump is kept on (PRD) or turned off (pure RD, no data points). PRD and RD used the same dose rates (6.4 krad min^{-1} at 30 krad, 24.6 krad min^{-1} at 450 krad). After measuring the degradation level at the end of irradiation, we follow the pump-induced PD or PB in the third phase. The latter approach the PDEL, as in Fig. 3. When degradation is stopped below the PDEL (30 krad), both YDF are less darkened in RD than in PRD conditions. Then the pump enhances darkening compared with pure RD. When induced losses exceed the PDEL (450 krad), RD yields more degradation than PRD. Then the pump slows down

the darkening build-up; it mitigates RD. The pump has therefore the same PD or PB action, according to the dose, during as after PRD (Fig. 2).

At the same pump power, the PDEL is ~0.11 cm^{-1} for K10 and ~8×10^{-3} cm^{-1} for Yb1200: the commercial fibre is 14 times more PD-resistant than our classic YDF. More strikingly, RD and PRD levels reached in K10 and Yb1200 at identical doses are proportionally scaled with respect to their respective PDEL. Since this homothetic connection holds for RD (x rays only, no pump), it is not be due primarily to the pump. The fact remains that the ratio of the RD level of K10 to that of Yb1200 is ~14 at each dose, nearly equal to the PDEL ratio. Obviously, the technique employed to harden the Yb1200 fibre against PD also makes this fibre RD-resistant. Unless the similarity between the PD and RD reduction factors stems from an astounding coincidence, we conclude that the hardening recipe has probably an effect on the trapping centers shared by PD and RD [5] and not on the PB efficiency of the pump.

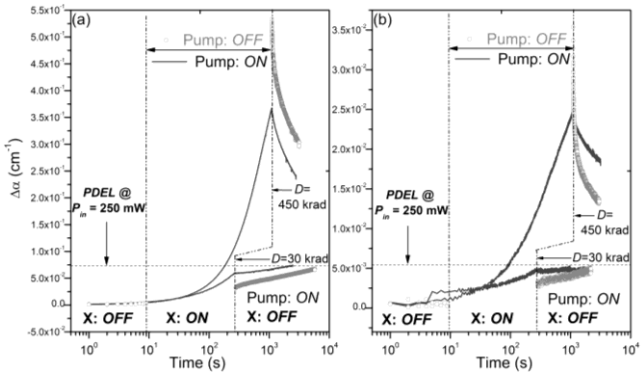

Fig. 4. Excess loss Δα at 976 nm, comparison between PRD and RD at 30 and 450 krad for the K10 (a) and Yb1200 (b) fibres. Pump power is P_{in} = 250 mW.

Under irradiation and pumping, the pump acts as a photo-bleacher as soon as the degradation level exceeds the PDEL. Due to the homothetic connection between K10 and Yb1200 fibres, the dose required to pass the two markedly different PDEL is the same. At long time, PB balances PRD and a PRD equilibrium level (PRDEL) is reached above the PDEL. Examples of transient PRD and PRDEL are shown in Fig. 5. The RD build-up is frozen at the PRDEL even if irradiation is continued. The strength of the RD mitigation by the pump and the PRDEL depend on the pump power, i.e. the PDEL, but also on the RD kinetics in relation to that of PD/PB, i.e. the dose rate.

The effect of a change in pump power at fixed dose rate is illustrated in Fig. 5. It compares transient and steady-state PD and PRD obtained on K10 samples at P_{in} = 250 and 115 mW. PRD was monitored for about 7 hours under irradiation at 7.2 krad min^{-1} to approach the PRDEL (total dose ~3 Mrad). PD was recorded for more than 28 hours. Increasing the pump power raises the PDEL from ~0.08 to ~0.1 [2]. Meanwhile the PRDEL lessens from ~0.83 to ~0.75 cm^{-1}. A higher pump power leads to an enhanced PB and hence to a strengthened 'restoring force' towards the PDEL. Therefore the fibre is more photo-darkened but less radiation-induced darkened. At very high pump power the PDEL and PRDEL are expected to merge. Then, the PRD resistance would be fully determined by the PD-resistance.

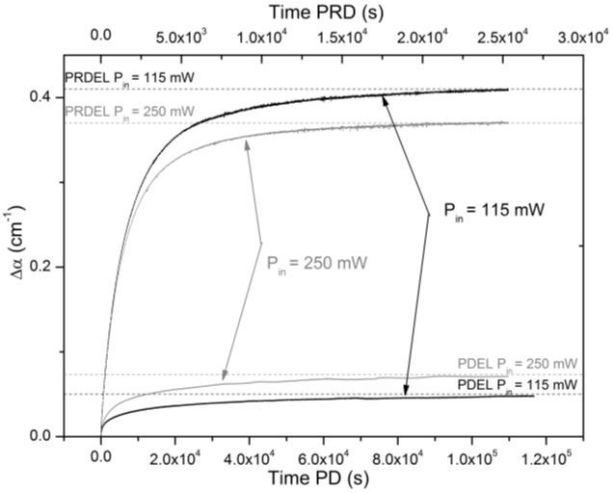

Fig. 5. Development of PD- and PRD-induced losses in K10 at 2 pump powers. The PRD dose is 3 Mrad.

PRD tests of Fig. 2 to 5 have been conducted at high dose rates leading to fast PRD build-up compared with PD. To characterize the competition between RD and PB when these processes come with closer kinetics, we examined the PRDEL evolution at decreasing dose rates but constant pump power P_{in} = 250 mW. In order to emphasize the PB action by the pump, we split a total dose of 900 krad in 1, 3, 6 and 12 equal fractions. Each fraction was given in PRD conditions at 43 krad min^{-1}. We observed a 75 min PB time between each fraction to achieve mean dose rates of about 5.3, 2.3 and 1.1 krad min^{-1} for the 3, 6 and 12 fraction runs respectively. Results are displayed in Fig. 6 for K10 (a) and for Yb1200 (b). The relevance of the procedure was checked on K10 by doing the measurement with a 5.3 krad min^{-1} constant dose rate. The corresponding curve is shown in Fig. 6, and its trend is well reproduced by the 3-fraction run. Induced losses oscillate around a mean tendency representative of the PRD build-up. The PRDEL sketched out from fractional irradiations is lowered and approaches the PDEL when the mean dose rate is decreased (constant dose 900 krad). It is difficult to achieve even lower mean dose rates, which would require too long experiments, so we cannot directly show the limit case where the PRDEL reaches the PDEL. However, the fractional irradiation protocol well highlights that PRDEL and PDEL must merge at sufficiently low dose rates. Then, RD will develop so slowly that the pump will have time to bleach the fibre "adiabatically" down to the PDEL as soon as darkening will slightly exceed this level. Such a regulation

around the PDEL is already clear in the first two fractions given to K10 in the 12 fraction irradiation test (Fig. 6(a)).

This work demonstrates and characterizes interaction modes between photo- and radiation-induced losses in YDF. The highlighted properties are general, holding for classic aluminosilicate YDF as well as state-of-the-art low-PD commercial YDF based on more sophisticated composition and elaboration technique. The radiation resistance of YDF should be tested under simultaneous pumping unless the observed degradation levels and dose rate dependence will not reproduce those really achieved in operation conditions. The lowered degradation we found at low dose rate rests on the action of the pump. An opposite trend might be measured in passive tests [7,10]. The remarkable interplay between PD and RD basically arises from the fact that both degradation types share the same color centers and therefore that pump-induced PB competes with both PD and RD. Even not reported in this letter focused on aluminosilicate fibers, this basic finding is found to hold in phosphorus co-doped fibers also. PD is added to RD at small ionizing doses, when the PRD level is below the PDEL. Conversely, PB prevails over PD as soon as the PRD level passes the PDEL. Then the pump mitigates RD and a PRDEL can be reached above a threshold dose from which the degradation is frozen. The PRDEL sets the worst degradation level achievable in PRD conditions and so the safest reference to be optimized to ensure the YDF resistance in operation conditions. According to Fig. 5 and 6, the PRDEL of a given fibre is determined by its intrinsic PD resistance, pump power (these two parameters set the PDEL), and dose rate. Although defined for pure PD, the PDEL turns out to be critical for the PRD resistance also. Low PDEL YDF will exhibit lower PRDEL than PD-sensitive ones due to more efficient PB by the pump. In fact the PDEL represents the minimum PRDEL value, reached at high pump power and/or low dose rate. Space based applications are precisely concerned with very low dose rates, in the range ~10^{-7} – 10^{-5} krad min^{-1}. This range is reported in insets of Fig. 6, where the PRDEL of the K10 and Yb1200 fibres (estimated from fractional irradiation runs) are plotted as a function of the mean dose rate. Data points roughly describe a power-law decay with decreasing dose rate, and extrapolation of this trend towards low dose rates (arrows) indicates that the PRDEL will be equal to the PDEL in space conditions. This statement is most probably correct though additional data points would be needed to refine the extrapolated cross-over dose rate where the PRDEL reach the PDEL. As a consequence, a PD-resistant YDF will be also RD-resistant in space-based applications. This is true at low dose, as that cumulated throughout a typical 15 year space mission around the Earth (~30 krad), but also for much higher doses that should be encountered in deeper space exploration missions (up to 150 krad) [11].

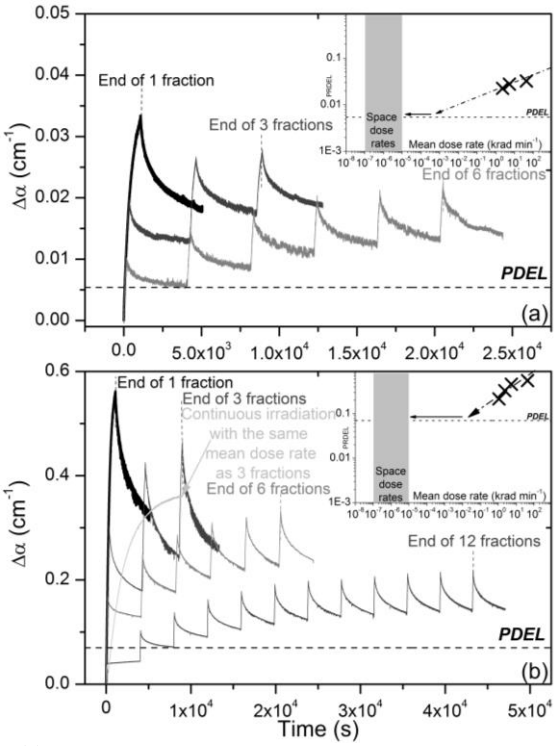

Fig. 6. (a) Excess loss Δα in K10 after a 900 krad X-ray dose given in 1, 3, 6 and 12 fractions. (b) Excess loss Δα in Yb1200 after a 900 krad X-ray dose given in 1, 3 and 6 fractions.

This work has been funded by the French National Research Agency (ANR) under grant #11-JS04-007-11. The authors gratefully acknowledge this support.

References.

1. A. Schwuchow, S. Unger, S. Jetschke, and J. Kirchhof, Applied Optics **53**, 1466 (2014).
2. S. Jetschke, S. Unger, U. Röpke and J. Kirchhof, Opt. Express **15**, 14838 (2007).
3. S. Rydberg and M. Engholm, Opt. Express 21, 6681 (2013).
4. H. Gebavi, S. Taccheo, D. Tregoat, A. Monteville, and T. Robin, Opt. Mater. Express 2, 1286 (2012).
5. F. Mady, M. Benabdesselam, and W. Blanc, Opt. Lett. **35**, 3542 (2010).
6. S. Girard, Y. Ouerdane, B. Tortech, C. Marcandella, T. Robin, B. Cadier, J. Baggio, P. Paillet, V. Ferlet-Cavrois, A. Boukenter, J.-P. Meunier, J. R. Schwank, M. R. Shaneyfelt, P. E. Dodd, and E. W. Blackmore, IEEE Trans. Nucl. Sci. **56**, 3293 (2009).
7. O. Gilard, J. Thomas, L. Troussellier, M. Myara, P. Signoret, E. Burov and M. Sotom, Appl. Opt. **51**, 2230 (2012).
8. S. Girard, A. Laurent, E. Pinsard, T. Robin, B. Cadier, M. Boutillier, C. Marcandella, A. Boukenter, and Y. Ouerdane, Opt. Lett. **39**, 2541 (2014).
9. N. Li, S. Yoo, X. Yu, D. Jain and J. K. Sahu, Photon. Technol. Lett. **26**, 115 (2014).
10. F. Mady, M. Benabdesselam, J.-B. Duchez, Y. Mebrouk and S. Girard, IEEE T. Nucl. Sci. **60**, 4341 (2013).
11. S. Campagnola and Y. Kawakatsu, J. Spacecraft Rockets **49**, 318 (2012).

1. Anka Schwuchow, Sonja Unger, Sylvia Jetschke, and Johannes Kirchhof, "Advanced attenuation and fluorescence measurement methods in the investigation of photodarkening and related properties of ytterbium-doped fibers," Appl. Opt. 53, 1466-1473 (2014).
2. Sylvia Jetschke, Sonja Unger, Ulrich Röpke, and Johannes Kirchhof, "Photodarkening in Yb doped fibers: experimental evidence of equilibrium states depending on the pump power," Opt. Express 15, 14838-14843 (2007)
3. S. Rydberg and M. Engholm, "Experimental evidence for the formation of divalent ytterbium in the photodarkening process of Yb-doped fiber lasers," Opt. Express 21, 6681-6688 (2013).
4. H. Gebavi, S. Taccheo, D. Tregoat, A. Monteville, and T. Robin, "Photobleaching of photodarkening in ytterbium doped aluminosilicate fibers with 633 nm irradiation," Opt. Mater. Express 2, 1286-1291 (2012).
5. Franck Mady, Mourad Benabdesselam, and Wilfried Blanc, "Thermoluminescence characterization of traps involved in the photodarkening of ytterbium-doped silica fibers," Opt. Lett. 35, 3541-3543 (2010).
6. S. Girard, Y. Ouerdane, B. Tortech, C. Marcandella, T. Robin, B. Cadier, J. Baggio, P. Paillet, V. Ferlet-Cavrois, A. Boukenter, J.-P. Meunier, J. R. Schwank, M. R. Shaneyfelt, P. E. Dodd, and E. W. Blackmore, "Radiation Effects on Ytterbium- and Ytterbium/Erbium-Doped Double-Clad Optical Fibers", IEEE Trans. Nucl. Sci. 56, 3293-3299 (2009).
7. Olivier Gilard, Jérémie Thomas, Laurent Troussellier, Mikhael Myara, Philippe Signoret, Ekaterina Burov, and Michel Sotom, "Theoretical explanation of enhanced low dose rate sensitivity in erbium-doped optical fibers," Appl. Opt. 51, 2230-2235 (2012).
8. S. Girard, A. Laurent, E. Pinsard, T. Robin, B. Cadier, M. Boutillier, C. Marcandella, A. Boukenter, and Y. Ouerdane, "Radiation-hard erbium optical fiber and fiber amplifier for both low- and high-dose space missions," Opt. Lett. 39, 2541-2544 (2014).
9. Li, N., Yoo, S., Yu, X., Jain, D., & Sahu, J. K., "Pump Power Depreciation by Photodarkening in Ytterbium-Doped Fibers and Amplifiers", IEEE PhotonicsTechnology Letters, 26(2), 115-118, (2014).
10. Mady, F.; Benabdesselam, M.; Duchez, J.-B.; Mebrouk, Y.; Girard, S., "Global View on Dose Rate Effects in Silica-Based Fibers and Devices Damaged by Radiation-Induced Carrier Trapping," Nuclear Science, IEEE Transactions on , vol.60, no.6, pp.4341,4348, Dec. 2013.
11. Campagnola, S. and Kawakatsu, Y., "Jupiter Magnetospheric Orbiter: Trajectory Design in the Jovian System", Journal of Spacecraft and Rockets, Vol. 49, No. 2, pp. 318-324, 2012.